The HKU Scholars Hub   The University of Hong Kong   香港大學學術庫

Title	An efficient marching-on-in-degree solution of transient multiscale EM scattering problems
Author(s)	He, Z; Chen, RS; Sha, W
Citation	IEEE Transactions on Antennas and Propagation, 2016, v. 64 n. 7, p. 3039-3046, article no. 7460917
Issued Date	2016
URL	http://hdl.handle.net/10722/234579
Rights	IEEE Transactions on Antennas and Propagation. Copyright © IEEE.; ©2016 IEEE. Personal use of this material is permitted. Permission from IEEE must be obtained for all other uses, in any current or future media, including reprinting/republishing this material for advertising or promotional purposes, creating new collective works, for resale or redistribution to servers or lists, or reuse of any copyrighted component of this work in other works.; This work is licensed under a Creative Commons Attribution-NonCommercial-NoDerivatives 4.0 International License.

An Efficient Marching-on-in-Degree Solution of Transient Multiscale EM Scattering Problems

Z. He, R. S. Chen, *Senior Member, IEEE*, Wei E. I. Sha, *Member, IEEE*

Abstract—**A marching-on-in-degree (MOD) based time-domain domain decomposition method (TD-DDM) is proposed to efficiently analyze the transient EM scattering from electrically large multiscale targets. The algorithm starts with an octree which divide the whole scattering target into several sub-domains. Then using the equivalence principle algorithm (EPA) each sub-domain is enclosed by an equivalence sphere, where both the RWG and BoR spatial basis functions are employed to expand the unknown currents. The interactions of the near-field sub-domains are calculated directly by the method of moments (MoM), while the far-field interactions can be converted to the interactions of corresponding equivalence spheres. This scheme implicitly satisfies the current continuity condition and the convergence can be accelerated as well. By harnessing the rotational symmetry of the equivalence spheres, the computational resources are reduced significantly compared to the traditional MOD method. Several numerical examples are presented to demonstrate the accuracy and efficiency of the proposed algorithm.**

Index Terms—**EM scattering, equivalence principle algorithm, time-domain domain decomposition method**

I. INTRODUCTION

Recently, the multiscale electromagnetic (EM) scattering problem has been an important research topic in computational electromagnetics society. The multiscale problem is extremely challenging for traditional numerical methods because of the bad convergence. A lot of numerical techniques were proposed to solve the problems with a high efficiency [1-7].

On the other hand, the transient EM scattering problems have been paid more and more attention due to its rich application. The time domain integral equation (TDIE) is widely used to analyze wideband EM responses from scatterers. There are two representative schemes for the TDIE, namely the marching-on-in-time (MOT) scheme [8] and marching-on-in-degree (MOD) scheme [9]. A great number of strategies have been proposed to speed up the two schemes, such as the multilevel plane wave time domain algorithm (PWTD) [10], the time domain adaptive integral method (TD-AIM) [11], the fast Fourier transform (FFT) [12], the UV

method [13], the adaptive cross approximate (ACA) algorithm [14] and so on. Unfortunately, all above-mentioned methods can not improve the convergence of the matrix equation, which will result in bad computational efficiency.

In this paper, we proposed an efficient MOD solution to the transient multiscale EM scattering problems. Firstly, the whole scattering target is divided into several sub-domains with an octree data structure and each sub-domain is enclosed by an equivalence sphere. Then the interactions between two near-field sub-domains are computed directly with the MoM, while the far-field interactions can be replaced by the interactions of their corresponding equivalence spheres (ES) using the equivalence principle algorithm (EPA). It should be noted that the current continuity condition can be satisfied implicitly by this technique. By using the rotationally symmetric property of the equivalence spheres, the computational resources are reduced significantly [15-18]. Moreover, the basis transformation technique is adopted between the RWG and BoR basis sets defined on the equivalence spheres. At last, both the inner iteration in each local sub-domain and the outer iteration of all the sub-domains are employed simultaneously to solve the whole system with a high convergence rate.

The remainder of the paper is organized as follows. The proposed algorithm is described in detail in Section II. In Section III, a series of numerical examples are given to demonstrate the accuracy and efficiency of the proposed method. At last, a conclusion is drawn in Section IV.

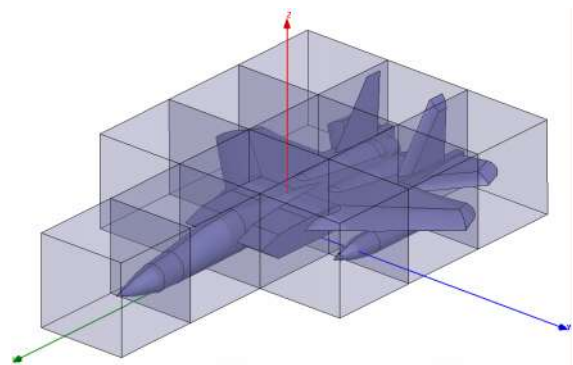## II. THEORY AND FORMULAS

A. Grouping Implementation

Fig. 1 Three-dimensional grouping sketch for an airplane (non-zero sub-domains).

As shown in Fig. 1, a cube is used to enclose the PEC airplane and the cube can be recursively decomposed into eight sub-cubes. More specifically, a scattering target can be divided into several sub-domains depending on an octree.
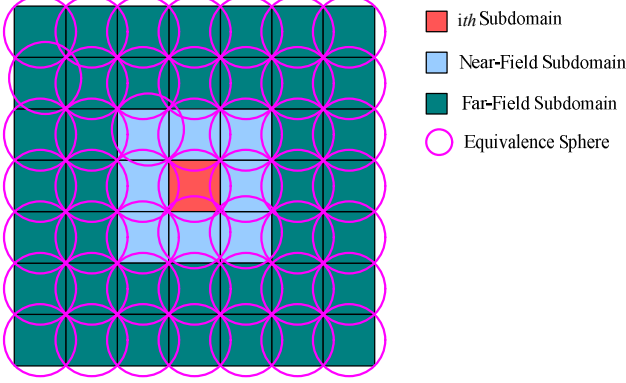

Fig. 2 Two-dimensional grouping sketch.

Each sub-domain is enclosed with an equivalence sphere with the same size. As shown in Fig. 2, the sub-domains are defined as the near-field interaction when their equivalence spheres are overlapping with each other. Otherwise, they are the far-field interaction.

Suppose a PEC target is illuminated by a plane wave in free space and it is divided into M sub-domains and the interaction in the ith sub-domain can be calculated as

$$\mathbf{Z}_{ii}\mathbf{I}_i = \mathbf{V}_i^{inc} + \sum_{j\in\Gamma_n}\mathbf{V}_{ij}^n + \sum_{j\in\Gamma_f}\mathbf{V}_{ij}^f$$
$$= \mathbf{V}_i^{inc} + \sum_{j\in\Gamma_n}\mathbf{Z}_{ij}\mathbf{I}_j + \sum_{j\in\Gamma_f}\mathbf{Z}_{ij}\mathbf{I}_j, \qquad (1)$$

where $\mathbf{Z}_{ii}$ is the self-acting matrix of the ith sub-domain, $\mathbf{I}_i$ and $\mathbf{I}_j$ represent the unknown current coefficients for the ith and jth sub-domain respectively, $\mathbf{Z}_{ij}$ denotes the interaction matrix between the ith and jth sub-domains, $\mathbf{V}_i^{inc}$ is the incident field for the ith sub-domain, Γ_n and Γ_f represent the near-field and far-field sub-domains.

For near-field interactions, the RWG basis functions on the scattering target are calculated directly with the MoM. Then the induced electric field of the ith sub-domain can be expressed in terms of the scattered electric current of the jth near-field sub-domain.

$$\mathbf{V}_{ij}^n(\mathbf{r},\tau) = \mathbf{Z}_{ij}\mathbf{I}_j = -\frac{\mu_0}{4\pi}\frac{\partial}{\partial t}\int_S\frac{\mathbf{J}_{PEC,j}^s(\mathbf{r}',\tau-R/c)}{R}dS$$
$$+ \frac{\nabla}{4\pi\varepsilon_0}\int_S\int_{-\infty}^{\tau-R/c}\frac{\nabla'\!\cdot\mathbf{J}_{PEC,j}^s(\mathbf{r}',\tau)}{R}d\tau dS$$
$$j\in\Gamma_n, \mathbf{r}\in ith\ subdomain, \mathbf{r}'\in jth\ subdomain$$
$$(2)$$

However, the interactions of any two far-field sub-domains are calculated by the ones between their corresponding equivalence spheres by using the EPA [3, 22-23]. In this way, the current continuity condition can be satisfied without tapping the basis functions. There are four steps for the calculation, namely outside-in propagation, solving for the current on the object, inside-out propagation, and translation operator.
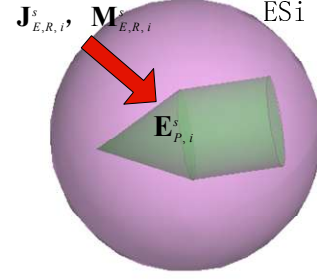
B. Outside-in propagation

Fig. 3 Outside-in propagation process.

The scattered electric current on the scattering target is discretized with the RWG spatial basis functions [1] and the weighted Laguerre polynomial as the temporal basis functions [9].

$$\mathbf{J}_{PEC,i}^s(\mathbf{r},\tau) = \sum_{n=1}^{N_s}\sum_{v=0}^{N_l}\left\{I_{PEC,n,v,i}\mathbf{f}_n(\mathbf{r})\varphi_v(s\tau)\right\}, \qquad (3)$$

where PEC stands for the perfect electric conductor, $I_{PEC,n,v,i}$ is the expansion coefficients of scattered electric current on the scattering target for basis function n and order v in the ith sub-domain, $\mathbf{f}_n(\mathbf{r})$ denotes the spatial RWG basis functions, $\varphi_v(s\tau)$ is served as the temporal basis functions, N_s and N_l represent the number of spatial and temporal basis functions, respectively.

The equivalent scattered electric/magnetic currents on ith equivalence sphere are expanded as the RWG spatial basis functions, which can be written as

$$\mathbf{J}_{ES,RWG,i}^s(\mathbf{r},\tau) = \sum_{n=1}^{N_s}\sum_{v=0}^{N_l}\left\{I_{ES,n,v,i}^J\mathbf{f}_n(\mathbf{r})\varphi_v(s\tau)\right\}, \qquad (4)$$

$$\mathbf{M}_{ES,RWG,i}^s(\mathbf{r},\tau) = \sum_{n=1}^{N_s}\sum_{v=0}^{N_l}\left\{I_{ES,n,v,i}^M\mathbf{f}_n(\mathbf{r})\varphi_v(s\tau)\right\}, \qquad (5)$$

where ES stands for equivalence sphere. $I_{ES,n,v,i}^J$ and $I_{ES,n,v,i}^M$ are the RWG expansion coefficients.

As shown in Fig. 3, the induced electric field on the scattering target for the ith sub-domain which is illuminated by the source on the ith equivalence sphere can be calculated as

$$\mathbf{E}_{PEC,i}^{s}(\mathbf{r},\tau) = \frac{\mu_0}{4\pi} \frac{\partial}{\partial t} \int_S \frac{\mathbf{J}_{ES,RWG,i}^{s}(\mathbf{r}',\tau-R/c)}{R} dS$$
$$- \frac{\nabla}{4\pi\varepsilon_0} \int_S \int_{-\infty}^{\tau-R/c} \frac{\nabla'\bullet\mathbf{J}_{ES,RWG,i}^{s}(\mathbf{r}',\tau)}{R} d\tau dS \quad (6)$$
$$- \frac{1}{4\pi} \int_S \nabla \times \frac{\mathbf{M}_{ES,RWG,i}^{s}(\mathbf{r}',\tau)}{R} dS$$

Where $R =| \mathbf{r} - \mathbf{r}' |$, ε_0 and μ_0 are respectively the permittivity and permeability in free space.

C. Solving for the current on the object

The scattered electric current on the PEC scattering target for the i*th* sub-domain can be computed as

$$\left[\mathbf{E}_{PEC,i}^{s}(\mathbf{r},\tau) \right]_{tan} = \left[\begin{array}{c} \dfrac{\mu_0}{4\pi} \dfrac{\partial}{\partial t} \int_S \dfrac{\mathbf{J}_{PEC,i}^{sca}(\mathbf{r}',\tau-R/c)}{R} dS \\[2mm] - \dfrac{\nabla}{4\pi\varepsilon_0} \int_S \int_{-\infty}^{\tau-R/c} \dfrac{\nabla'\bullet\mathbf{J}_{PEC,i}^{sca}(\mathbf{r}',\tau)}{R} d\tau dS \end{array} \right]_{tan} \quad (7)$$
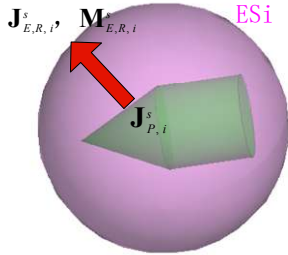
D. Inside-out propagation

Fig. 4 Inside-out propagation process.

As shown in Fig. 4, the induced equivalent scattered electric/magnetic current on i *th* equivalence sphere is obtained

$$\mathbf{J}_{ES,RWG,i}^{s}(\mathbf{r},\tau) = \hat{n}(\mathbf{r}) \times \frac{1}{4\pi} \int_S \nabla \times \frac{\mathbf{J}_{PEC,i}^{s}(\mathbf{r}',\tau)}{R} dS \quad (8)$$

$$\mathbf{M}_{ES,RWG,i}^{s}(\mathbf{r},\tau) = \hat{n}(\mathbf{r}) \times \left\{ \begin{array}{c} \dfrac{\mu_0}{4\pi} \dfrac{\partial}{\partial t} \int_S \dfrac{\mathbf{J}_{PEC,i}^{S}(\mathbf{r}',\tau-R/c)}{R} dS - \\[2mm] \dfrac{\nabla}{4\pi\varepsilon_0} \int_S \int_{-\infty}^{\tau-R/c} \dfrac{\nabla'\bullet\mathbf{J}_{PEC,i}^{s}(\mathbf{r}',\tau)}{R} d\tau dS \end{array} \right\} \quad (9)$$

where $\hat{n}(\mathbf{r})$ is the outward normal unit vector of the i *th* equivalence sphere.
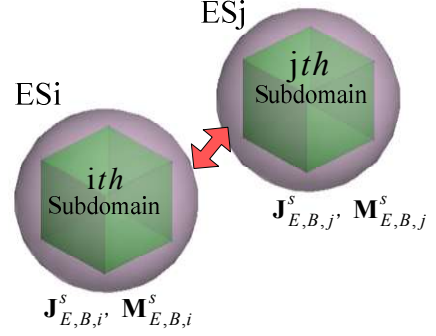
E. Translation operator

Fig. 5 Interaction between two far-field subdomains.

For the translation operator, the BoR basis functions [19-21] are used to discretize the equivalence sphere and can be expressed as

$$\mathbf{J}_{ES,BoR,i}^{s}(\mathbf{r},\tau) = \sum_{\alpha=-Mod}^{Mod} \sum_{n=1}^{N_s} \sum_{v=0}^{N_l} \left\{ \left[\begin{array}{c} I_{ES,\alpha,n,v,i}^{J,t}\mathbf{f}_{\alpha,n}^{t}(\mathbf{r}) \\ +I_{ES,\alpha,n,v,i}^{J,\varphi}\mathbf{f}_{\alpha,n}^{\varphi}(\mathbf{r}) \end{array} \right] \varphi_v(s\tau) \right\} \quad (10)$$

$$\mathbf{M}_{ES,BoR,i}^{s}(\mathbf{r},\tau) = \sum_{\alpha=-Mod}^{Mod} \sum_{n=1}^{N_s} \sum_{v=0}^{N_l} \left\{ \left[\begin{array}{c} I_{E,\alpha,n,v,i}^{M,t}\mathbf{f}_{\alpha,n}^{t}(\mathbf{r}) \\ +I_{E,\alpha,n,v,i}^{M,\varphi}\mathbf{f}_{\alpha,n}^{\varphi}(\mathbf{r}) \end{array} \right] \varphi_v(s\tau) \right\} \quad (11)$$

where $I_{ES,\alpha,n,v,i}^{J,t}$, $I_{ES,\alpha,n,v,i}^{M,t}$, $I_{ES,\alpha,n,v,i}^{J,\varphi}$ and $I_{ES,\alpha,n,v,i}^{M,\varphi}$ are the BoR expansion coefficients of the i*th* equivalence sphere for mode α , basis function n and order v . $\mathbf{f}_{\alpha,n}^{t}(\mathbf{r})$ and $\mathbf{f}_{\alpha,n}^{\varphi}(\mathbf{r})$ denote the spatial basis functions in the longitudinal and azimuthal direction, respectively.

Therefore, the RWG-based electric/magnetic currents on i *th* equivalence sphere should be converted into the BoR-based ones. Moreover, the coordinate transformation technique is adopted to transform the current coefficients among two different coordinate systems [22].

$$\left\langle \mathbf{J}_{ES,BoR,i}^{s}(\mathbf{r},\tau),\mathbf{f}_{\alpha,n}^{\gamma}(\mathbf{r}) \right\rangle = \left\langle \mathbf{J}_{ES,RWG,i}^{s}(\mathbf{r},\tau),\mathbf{f}_{\alpha,n}^{\gamma}(\mathbf{r}) \right\rangle \quad (12)$$

$$\left\langle \mathbf{M}_{ES,BoR,i}^{s}(\mathbf{r},\tau),\mathbf{f}_{\alpha,n}^{\gamma}(\mathbf{r}) \right\rangle = \left\langle \mathbf{M}_{ES,RWG,i}^{s}(\mathbf{r},\tau),\mathbf{f}_{\alpha,n}^{\gamma}(\mathbf{r}) \right\rangle \quad (13)$$

where $\gamma = t, \varphi$, $\left\langle \ , \ \right\rangle$ represents the inner-product operation.

Similarly, the BoR-based induced equivalent scattered electric/magnetic currents can also be converted into the RWG-based currents by using the following equations.

$$\left\langle \mathbf{J}_{ES,RWG,i}^{s}(\mathbf{r},\tau),\mathbf{f}_{n}(\mathbf{r}) \right\rangle = \left\langle \mathbf{J}_{ES,BoR,i}^{s}(\mathbf{r},\tau),\mathbf{f}_{n}(\mathbf{r}) \right\rangle \quad (14)$$

$$\left\langle \mathbf{M}_{ES,RWG,i}^{s}(\mathbf{r},\tau),\mathbf{f}_n(\mathbf{r})\right\rangle = \left\langle \mathbf{M}_{ES,BoR,i}^{s}(\mathbf{r},\tau),\mathbf{f}_n(\mathbf{r})\right\rangle \quad (15)$$

Suppose the $i\,th$ and $j\,th$ sub-domains are far-field interactions, as shown in Fig. 5. The interactions of two far-field sub-domains can be computed as follows.

$$\mathbf{J}_{ES,BoR,i}^{s}(\mathbf{r},\tau) = -\hat{n}(\mathbf{r}) \times \frac{1}{4\pi}\int_S \nabla \times \frac{\mathbf{J}_{ES,BoR,j}^{s}(\mathbf{r}',\tau)}{R}dS$$
$$+\frac{1}{\eta^2}\hat{n}(\mathbf{r}) \times \left\{ \begin{array}{l} \dfrac{\mu_0}{4\pi}\dfrac{\partial}{\partial t}\int_S \dfrac{\mathbf{M}_{ES,BoR,j}^{s}(\mathbf{r}',\tau-R/c)}{R}dS - \\[2mm] \dfrac{\nabla}{4\pi\varepsilon_0}\int_S \int_{-\infty}^{\tau-R/c}\dfrac{\nabla'\cdot\mathbf{M}_{ES,BoR,j}^{s}(\mathbf{r}',\tau)}{R}d\tau dS \end{array} \right\} \quad (16)$$

$$\mathbf{M}_{ES,BoR,i}^{s}(\mathbf{r},\tau) = -\hat{n}(\mathbf{r}) \times \frac{1}{4\pi}\int_S \nabla \times \frac{\mathbf{M}_{ES,BoR,j}^{s}(\mathbf{r}',\tau)}{R}dS$$
$$-\hat{n}(\mathbf{r}) \times \left\{ \begin{array}{l} \dfrac{\mu_0}{4\pi}\dfrac{\partial}{\partial t}\int_S \dfrac{\mathbf{J}_{ES,BoR,j}^{s}(\mathbf{r}',\tau-R/c)}{R}dS - \\[2mm] \dfrac{\nabla}{4\pi\varepsilon_0}\int_S \int_{-\infty}^{\tau-R/c}\dfrac{\nabla'\cdot\mathbf{J}_{ES,BoR,j}^{s}(\mathbf{r}',\tau)}{R}d\tau dS \end{array} \right\} \quad (17)$$

For the far-field interactions, the unknowns are expanded with spatial basis functions defined on the boundary curve and Fourier series in the azimuthal direction due to the rotationally symmetric property of the equivalence sphere. Therefore, both the memory requirement and the CPU time can be reduced significantly. It should be noted that the outer iteration among the far-filed sub-domains is finished when the induced scattered electric current on the scattering target becomes stable.

III. NUMERICAL EXAMPLES

In this section, several numerical results are presented to demonstrate the effectiveness of the proposed solver. All numerical results are tested on a Dell workstation with 40 CPUs and 512 GB memory. The mesh sizes of both the RWG and BoR basis functions for the equivalence sphere are $0.1\lambda_{min}$, where λ_{min} is the wavelength at the maximum frequency. The incident wave is a modulated Gaussian pulse and is defined as

$$\mathbf{E}^{i}(\mathbf{r},t) = \hat{\mathbf{x}}\cos[2\pi f_0(t-R/c)]\bullet$$
$$\exp[-\frac{(t-R/c-t_p)^2}{2\sigma^2}] \quad (18)$$

where f_0 is the center frequency, $\sigma = 6/(2\pi f_{bw})$, f_{bw} represents the bandwidth of the Gaussian impulse, and t_p is the time delay.

A. Accuracy and computational complexity

Firstly, the transient EM scattering from a PEC sphere with the radius of 0.7 m is investigated with the center frequency of 150 MHz and the pulse width of 300 MHz. The incident plane

wave is fixed at $\theta^{inc} = 0^{\circ}$, $\varphi^{inc} = 0^{\circ}$ and the time delay of the modulated Gaussian pulse is 4.5 lm. The mesh size for this sphere is 0.1 m. The unknown scattered electric current on the PEC sphere is expanded with 1836 spatial basis functions and 50 temporal basis functions. The whole computational domain is divided into 64 sub-domains with the size of $0.4\,\text{m} \times 0.4\,\text{m} \times 0.4\,\text{m}$. It should be noted that there are 48 nonempty sub-domains. Each of them is enclosed with an equivalence sphere with the radius of 0.4 m. Each equivalence sphere is discretized into 606 RWG and 16 BoR spatial basis functions. Four Fourier modes are needed in this computation. As shown in Fig. 6, the bistatic RCS results are compared between the proposed method and the Mie Series at several frequencies. It can be seen that there is a good agreement between them. Moreover, the backward scattered field for the proposed method is compared with the one of the traditional MOD method in Fig. 7.

Additionally, the computational complexity of the proposed method is investigated. Only the $0\,th$ degree of the temporal basis function is simulated for the sake of available memory. Both the memory requirement and average CPU time per degree with 825, 1311, 1836 and 2919 spatial unknowns are shown in Fig. 8. It can be seen that the complexity of the proposed method scales as $O(N)$.
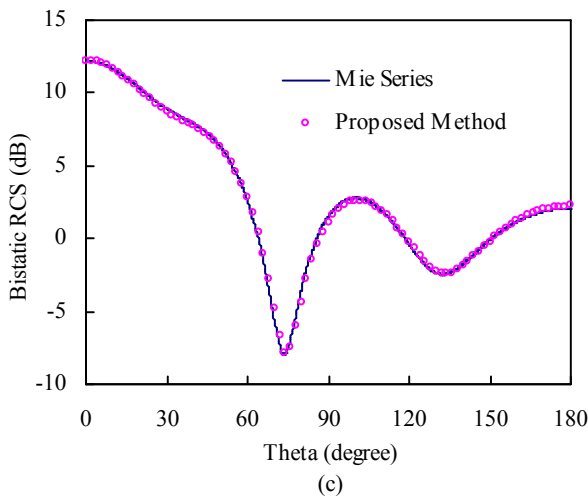
(a)

(b)

(c)
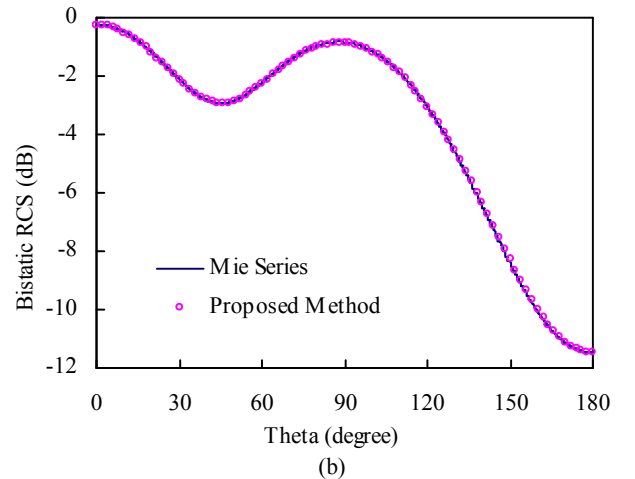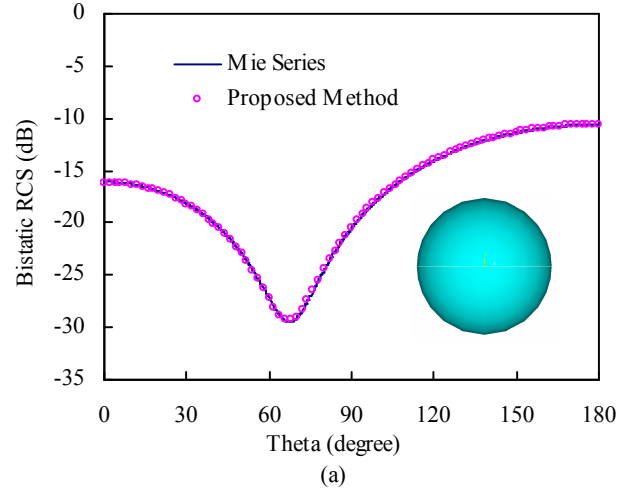
Fig. 6 Bistatic RCS results of a PEC sphere:
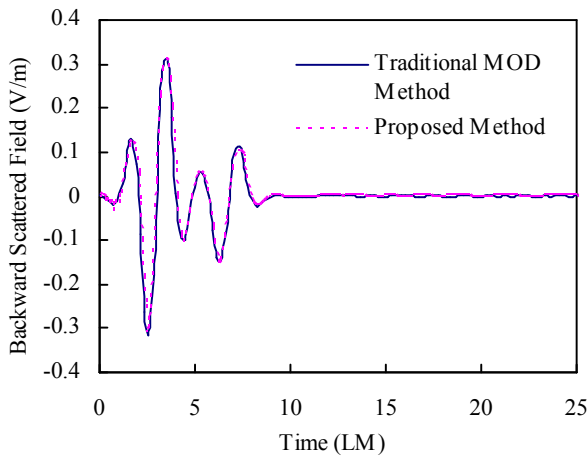(a) f=50MHz, (b) f=150MHz, (c) f=250MHz.

Fig. 7 The backward scattered field for a PEC sphere.
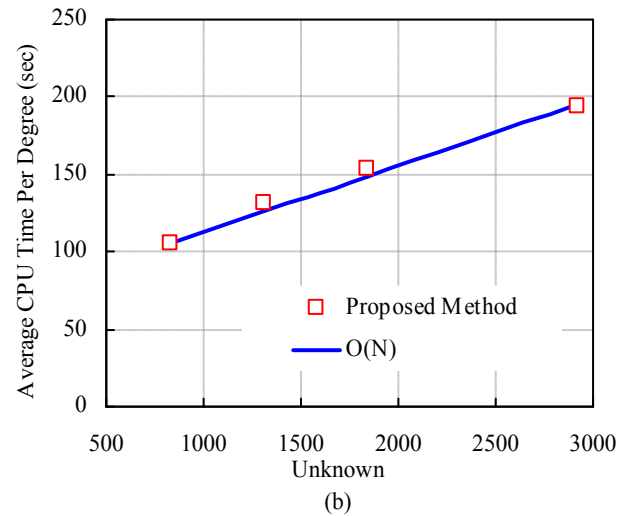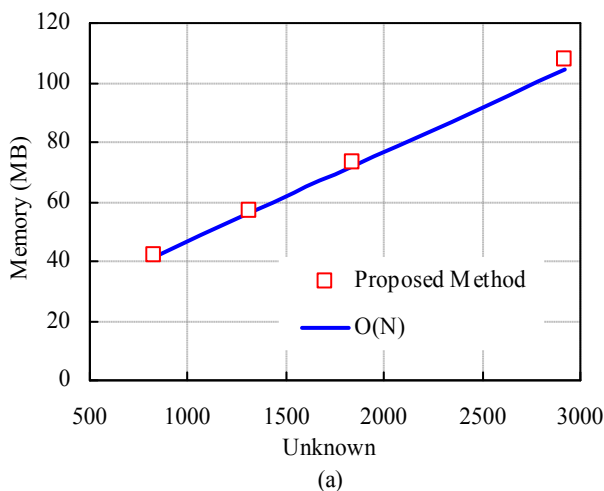

(a)

(b)

Fig. 8 (a) Memory requirement of PEC sphere versus spatial unknowns,
(b) Average CPU time per degree of PEC sphere versus spatial unknowns.

B. Convergence performance and optimal grouping scheme

Secondly, we consider the transient EM scattering from a ring with the inner radius of 1.2 m and the outer radius of 1.5 m. The time delay of the modulated Gaussian pulse is set to be 4.0 lm with the center frequency of 150 MHz and the pulse width of 300 MHz, where lm represents light meter and 1(lm) = 1/3.0e8. In this numerical example, 12132 spatial basis functions and 80 temporal basis functions are adopted with four modal equations to be solved. The whole computational domain is divided into 64 sub-domains with the size of $0.8 \text{ m} \times 0.8 \text{ m} \times 0.8 \text{ m}$ and there are 12 nonempty sub-domains. The radius of the equivalence sphere is 0.75 m and the equivalence sphere is discretized into 639 RWG and 24 BoR spatial basis functions. The meshes and the grouping of the ring are shown in Fig. 9. The mesh size of $0.05\lambda_{\min}$ is adopted to both the top and the down faces and $0.08\lambda_{\min}$ for the sides. As shown in Fig. 10, bistatic RCS results of the proposed method at several frequencies are given and compared with the traditional MOD method.

Moreover, the convergences for the first order are compared between them in Fig. 11 and the numbers of convergence for each order are given in Fig. 12. Additionally, the convergence performance is tested for the multiscale problem. The part of the ring is meshed densely. As shown in Fig. 13, the iteration number of the proposed method is compared with the traditional MOD method versus the ratio of the maximum mesh size over the minimum mesh size. It can be found that the proposed method is much more stable for the multiscale problems.

At last, the computational resources for different grouping schemes are given in Table 1. The memory requirement can be reduced with the size of sub-domains decreasing. However, more CPU time is needed when the grouping size is too small or too big. Some additional propagation operators are needed to be calculated when the grouping size is big, which will result in bad efficiency. On the other hand, a lot of CPU time is needed

for the calculation of translation operators when the grouping size is small. It can be concluded from the numerical results that higher efficiency can be obtained when there is a good balance between the numbers of near-field and far-field interactions. Generally speaking, the optimal grouping scheme can be achieved when the number of BoR unknowns on the equivalence sphere is much smaller than the one of RWG unknowns on the scattering target in this sub-cube and the total number of nonempty sub-domains is less than 30 at the same time.
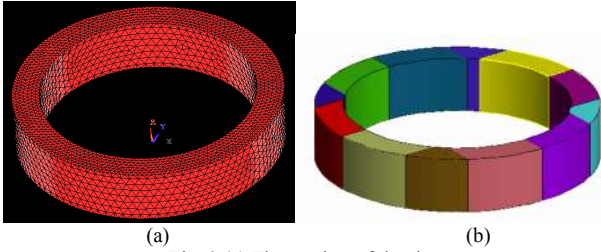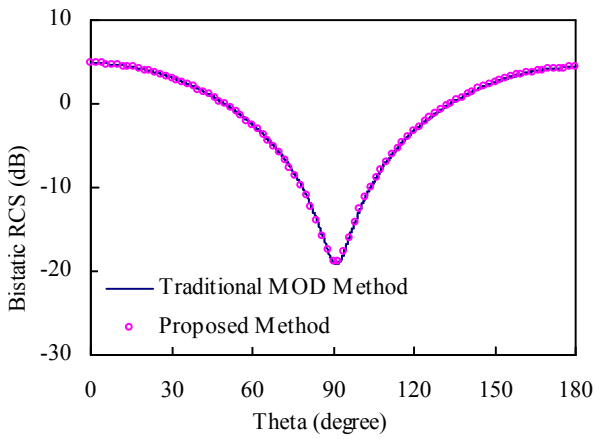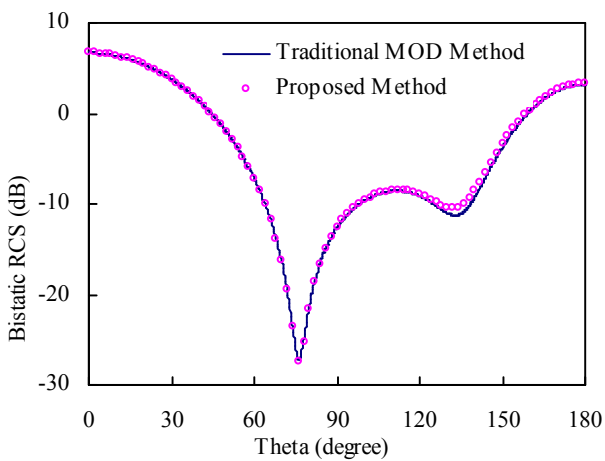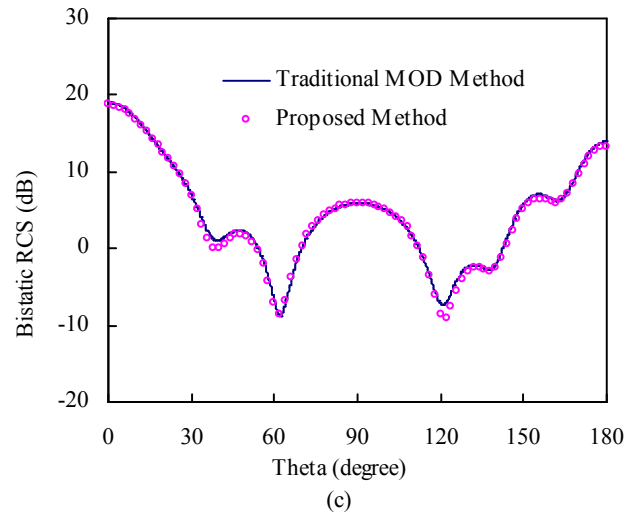

(a)   (b)

Fig. 9 (a) The meshes of the ring
(b) The grouping of the ring (one color stands one group).

(c)

Fig. 10 Bistatic RCS results of the ring:
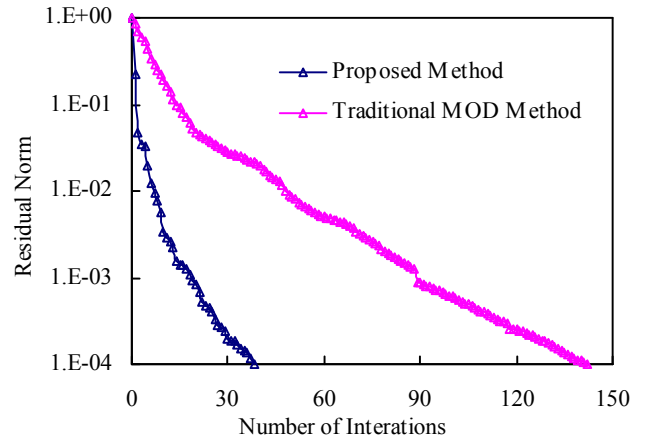(a) f=50MHz, (b) f=150MHz, (c) f=250MHz.

(a)

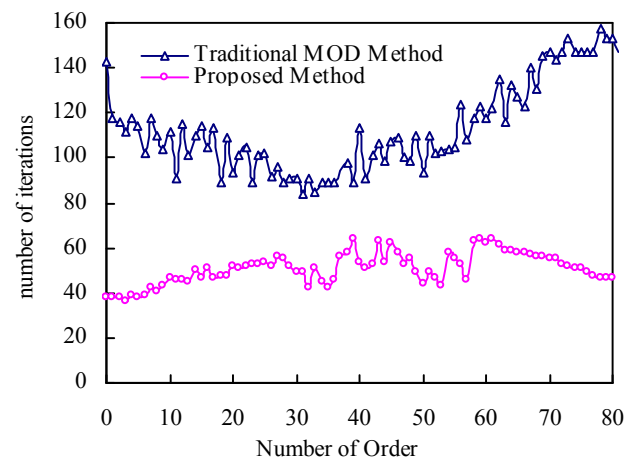Fig. 11 Convergence history of the first order for the ring.

(b)

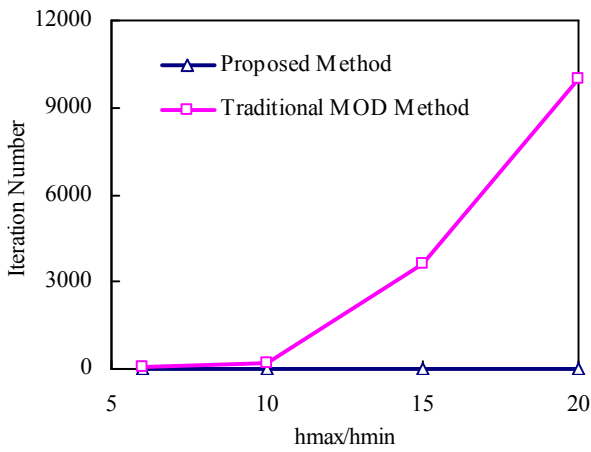Fig. 12 Number of iteration versus temporal order.

Fig. 13 Iteration number versus the ratio of the maximum mesh size over the minimum mesh size.

Table 1 Comparisons of different grouping schemes

Size of Sub-domains (m)	No. of Sub-domains (Total/Nonempty)	Total CPU Time (h)	Memory Requirement (GB)
2.8	8/4	12.5	39.7
1.5	64/12	8.22	32.9
0.8	512/88	49.3	15.4

(a)   (b)   (c)

Fig. 14 (a) The geometry of the missile model
(b) The grouping of the missile model (one color stands one group)
(c) The mesh of the missile model.

C. Computational efficiency

Thirdly, a missile model is analyzed by the proposed method with the incident plane wave fixed at $\theta^{inc} = 0°$, $\varphi^{inc} = 0°$. The geometry, the grouping scheme and the mesh of the missile model are given in Fig. 14. It can be seen that the meshes are nonuniform on the surface. The mesh size of 0.1 m is adopted to the cylinder and 0.04 m for the wings. In this numerical example, the center frequency of modulated Gaussian pulse is 150 MHz, the pulse width is 300 MHz and the time delay is 5.0 lm. This problem is discretized into 18213 spatial basis functions and 80 temporal basis functions and two Fourier modes are needed. The whole computational domain is divided into 512 subdomains with the size of 1.4 m × 1.4 m × 1.4 m and there are 5 nonempty subdomains. The radius of the equivalence sphere is 1.3m and the equivalence sphere is discretized into 1329 RWG and 36 BoR spatial basis functions. As shown in Fig. 15, bistatic RCS results at several frequencies are compared between the proposed method and the traditional MOD method. Moreover, the computational resources are listed in Table 2.
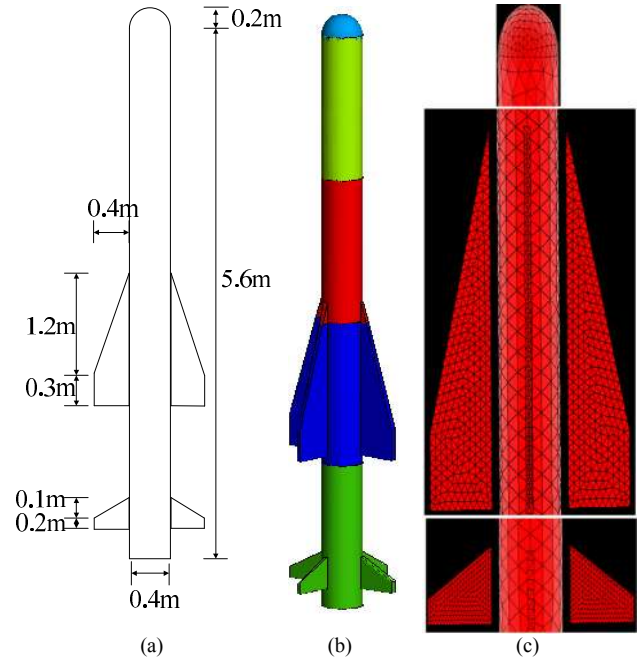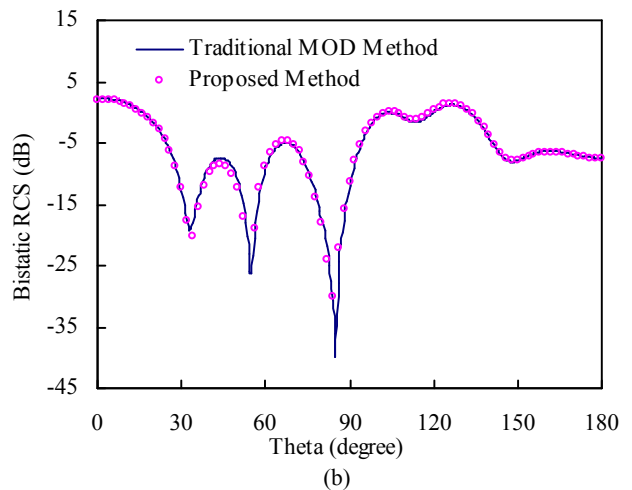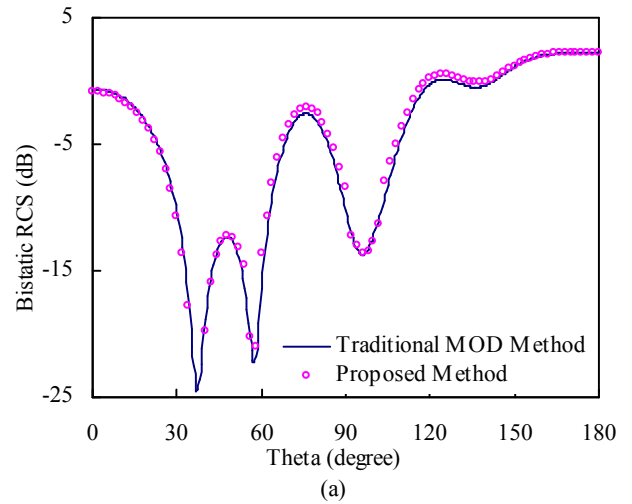

(a)

(b)
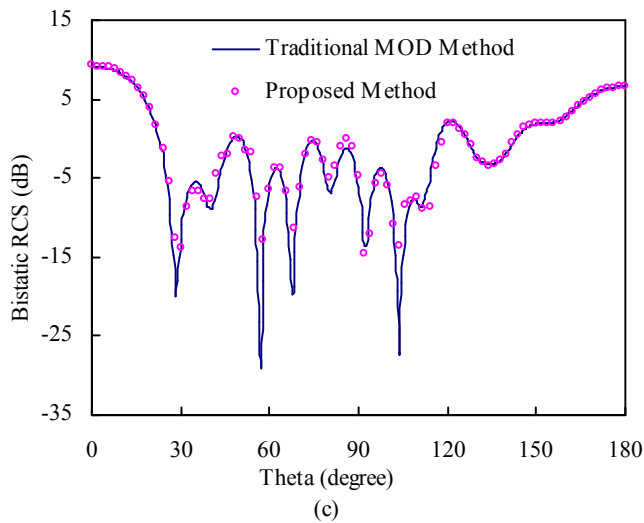
Fig. 15 Bistatic RCS results of the missile model:
(a) f=50MHz, (b) f=150MHz, (c) f=250MHz.

Table 2 Comparison of the average number of iteration, memory requirement and the total CPU time for the missile model.

Methods	Average Number of Iteration	Memory Requirement (GB)	Total CPU Time (h)
Traditional MOD Method	602	197.8	17.8
Proposed Method	8	32.1	13.1

IV. CONCLUSION

A novel marching-on-in-degree solver is proposed to analyze the transient multiscale EM scattering problems. The whole computational region is divided into several sub-domains and each sub-domain is enclosed with an equivalence sphere. Then the interactions of the far-field sub-domains are converted to the interactions of their corresponding equivalence spheres with BoR basis functions. Therefore, compared with the traditional MOD method, the memory requirement is reduced significantly and good convergence is obtained by the proposed method. Numerical examples are presented to demonstrate the validity and efficiency of the proposed method.

REFERENCES

[1] S. M. Rao, D. R. Wilton, and A. W. Glisson, "Electromagnetic scattering by surfaces of arbitrary shape," *IEEE Trans. Antennas Propag.,* vol. 30, pp. 409–418, 1982.

[2] J. M. Song, C. C. Lu, and W. C. Chew, "Multilevel fast multipole algorithm for electromagnetic scattering by large complex objects," *IEEE Trans. Antennas and Propag.,* vol. 45, pp. 1488–1493, 1997.

[3] M. K. Li and W. C. Chew, "Multiscale simulation of complex structures using equivalence principle algorithm with high-order field point sampling scheme," *IEEE Trans. Antennas Propag.,* vol. 56, pp. 2389–2397, 2008.

[4] F. Vipiana, M. A. Francavilla, and G. Vecchi, "EFIE modeling of high definition multiscale structures," *IEEE Trans. Antennas Propag.,* vol. 58, pp. 2362–2374, 2010.

[5] Z. Peng, X. C. Wang, and J. F. Lee, "Integral equation based domain decomposition method for solving electromagnetic wave scattering from non-penetrable objects," *IEEE Trans. Antennas Propag.,* vol. 59, pp. 3328–3338, 2011.

[6] M. A. Francavilla, F. Vipiana, G. Vecchi, and D. R. Wilton, "Hierarchical fast MoM solver for the modeling of large multiscale wire-surface structures," *IEEE Antennas Wireless Propag. Lett.,* vol. 11, pp. 1378–1381, 2012.

[7] Z. Peng, K. H. Lim, and J. F. Lee, "Nonconformal domain decomposition methods for solving large multiscale electromagnetic scattering problems," *IEEE Trans. Antennas Propag.,* vol. 101, pp. 298–319, 2013.

[8] B. Shanker, A. A. Ergin, K. Ayügn, and E. Michielssen, "Analysis of transient electromagnetic scattering from closed surfaces using a combined field integral equation," *IEEE Trans. Antennas Propag.,* vol. 48, pp. 1064-1074, 2000.

[9] Y. S. Chung, T. K. Sarkar, B. H. Jung, M. Salazar-Palma, Z. Ji, S. M. Jang, and K. J. Kim, "Solution of time domain electric field integral equation using the Laguerre polynomials," *IEEE Trans. Antennas Propag.,* vol. 52, pp. 2319-2328. 2004.

[10] B. Shanker, A. A. Ergin, M. Lu, and E. Michielssen, "Fast analysis of transient electromagnetic scattering phenomena using the multilevel plane wave time domain algorithm," *IEEE Trans. Antennas Propag.,* vol. 51, pp. 628-641, 2003.

[11] A. E. Yilmaz, J. M. Jin, and E. Michielssen, "Time domain adaptive integral method for surface integral equations," *IEEE Trans. Antennas Propag.,* vol.52, pp. 2692–2708, 2004.

[12] M. D. Zhu, X. L. Zhou, W. Y. Yin, "An adaptive marching-on-in-order method with FFT-Based blocking scheme," *IEEE Antennas Wireless Propag. Lett.,* vol. 9, pp. 436-439, 2010.

[13] Q. Q. Wang, Y. F. Shi, M. M. Li, Z. H. Fan, R. S. Chen, and M. Y. Xia, "Analysis of transient electromagnetic scattering using UV method enhanced time-domain integral equations with Laguerre polynomials," *Microw. Opt. Technol. Lett.,* vol. 53, pp. 158–163, 2011.

[14] H. H. Zhang, Q. Q. Wang, Y. F. Shi, and R. S. Chen, "Efficient marching-on-in-degree solver of time domain integral equation with adaptive cross approximation algorithm-singular value decomposition," *Appl. Comput. Electromagn. Soc. J.,* vol. 27, pp. 475–482, 2012.

[15] W. M. Yu, D. G. Fang, and Z. Chen, "Marching-on-in-degree based time-domain magnetic field integral equation method for bodies of revolution," *Microwave and Wireless Components Letters, IEEE*, vol. 17, no.12, pp. 813-815, 2007.

[16] Z. He, H. H. Zhang, and R. S. Chen, "Parallel Marching-on-in-Degree Solver of Time-Domain Combined Field Integral Equation for Bodies of Revolution Accelerated by MLACA," *IEEE Trans. Antennas Propag.,* vol. 63, no. 8, pp. 3705-3710, 2015.

[17] Z. He, Z. H. Fan, D. Z. Ding, R. S. Chen, "Solution of PMCHW Integral Equation for Transient Electromagnetic Scattering from Dielectric Body of Revolution," *IEEE Trans. Antennas Propag.*, vol. 63, no. 11, pp. 5124-5129, 2015.

[18] Z. H. Fan, Z. He, R. S. Chen, "Marching-on-in-degree Solution of the Transient Scattering from Multiple Bodies of Revolution," *IEEE Trans. Antennas Propag.*, vol. 64, no. 1, pp. 321-326, 2015.

[19] M. Andreasen, "Scattering from bodies of revolution," *IEEE Trans. Antennas Propagat.*, vol. 13, no.2, pp. 303-310, Mar. 1965.

[20] J. R. Mautz and R. F. Harrington, "Radiation and scattering from bodies of revolution," *Appl. Sci. Res*, vol. 20, pp. 405-435, Jun. 1969.

[21] W. C. Gibson. The method of moments in electromagnetics. London: *Taylor & Francis Group,* 2008.

[22] T. Su, L. Du, and R. S. Chen, "Electromagnetic scattering for multiple PEC bodies of revolution using equivalence principle algorithm," *IEEE Trans. Antennas Propag.,* vol. 62, no. 5, pp. 2736–2744, 2014.

[23] M. K. Li and W. C. Chew, L. J. Jiang, "A domain decomposition scheme based on equivalence theorem," *Microw. Opt. Technol. Lett.,* vol. 48, pp. 1853–1857, 2006.

Z. He received the B.Sc. degree in Electronic Information Engineering from the School of Electrical Engineering and Optical Technique, Nanjing University of Science and Technology, Nanjing, China, in 2011.

She is currently working towards the PhD degree in electromagnetic fields and microwave technology at the School of Electrical Engineering and optical technique, Nanjing University of Science and Technology. Her research interests include antenna, RF-integrated circuits, and computational electromagnetics.

R. S. Chen (M'01) was born in Jiangsu, China. He received the B.Sc. and M.Sc. degrees from the Department of Radio Engineering, Southeast University, China, in 1987 and 1990, respectively, and the PhD degree from the Department of Electronic Engineering, City University of Hong Kong, in 2001.

He joined the Department of Electrical Engineering, Nanjing University of Science and Technology (NJUST), China, where he became a Teaching Assistant in 1990 and a Lecturer in 1992. Since September 1996, he has been a Visiting Scholar with the Department of Electronic Engineering, City University of Hong Kong, first as Research Associate, then as a Senior Research Associate in July 1997, a Research Fellow in April 1998, and a Senior Research Fellow in 1999. From June to September 1999, he was also a Visiting Scholar at Montreal University, Canada. In September 1999, he was promoted to Full Professor and Associate Director of the Microwave and Communication Research Center in NJUST, and in 2007, he was appointed as the Head of the Department of Communication Engineering, NJUST. He was appointed as the Dean in the School of Communication and Information Engineering, Nanjing Post and Communications University in 2009. And in 2011 he was appointed as Vice Dean of the School of Electrical Engineering and Optical Technique, NJUST. Currently, he is a principal investigator of more than 10 national projects. His research interests mainly include computational electromagnetics, microwave integrated circuit and nonlinear theory, smart antenna in communications and radar engineering, microwave material and measurement, RF-integrated circuits, etc. He has authored or coauthored more than 260 papers, including over 180 papers in international journals.

Prof. Chen is an expert enjoying the special government allowance, member of Electronic Science and Technology Group, Fellow of the Chinese Institute of Electronics (CIE), Vice-Presidents of Microwave Society of CIE and IEEE MTT/APS/EMC Nanjing Chapter and an Associate Editor for the International Journal of Electronics. He was also the recipient of the Foundation for China Distinguished Young Investigators presented by the China NSF, a Cheung Kong Scholar of the China Ministry of Education, New Century Billion Talents Award. Besides, he received several Best Paper Awards from the National and International Conferences and Organizations. He serves as the reviewer for many technical journals, such as the IEEE Transactions on Antennas and Propagation, the IEEE Transactions on Microwave Theory and Techniques, Chinese Physics, etc.

Wei E. I. Sha (M'09) received the B.S. and Ph.D. degrees in electronic engineering at Anhui University, Hefei, China, in 2003 and 2008, respectively. From July 2008 to May 2012, he was a Postdoctoral Research Fellow in the Department of Electrical and Electronic Engineering at the University of Hong Kong, where he is now a Research Assistant Professor.

Dr. Sha has co-authored two books respectively on wavelet theory and finite-difference time-domain method. He has published 70 peer-reviewed journal papers included in Web of Science Core Collection. He also contributed to four book chapters at Springer, CRC Press and InTech Publishers. Dr. Sha is an IEEE member and an OSA member. He has served as the committee member or session chair of several international conferences including PIERS 2016, ICCEM 2016, IMWS-AMP 2015, EICT 2015, ICSPS 2011, etc. He has been serving as the reviewers of IEEE, OSA, AIP, APS and Nature Publishing Group journals. He also served as the book proposal reviewers for CRC Press and Bentham Science publishers.

He received the Second Prize and First Prize of National Postgraduates Mathematical Contest in Modeling, respectively in 2006 and 2007. He was awarded Chinese Youth Science and Technology Innovation Prize in 2007. He and his collaborators received Research Output Prize at the University of Hong Kong in 2013. In 2015, he was awarded Second Prize of Natural Science from Anhui Province Government. He and his students received Second Place of Best Student Paper at PIERS 2014, First Place of Best Student Paper at ACES 2014, and Best Student Paper at NCMMW 2015. In 2014, he was awarded Outstanding Reviewer of Journal of Computational Physics.

He engages in theoretical and computational research in electromagnetics and optics, focusing on the multiphysics and interdisciplinary research. The research topics are inspired by applications in several areas including solar energy, microwave/optical communication, sensing/detection, and quantum information. His research involves fundamental and applied aspects in plasmonics, emerging photovoltaics, metasurfaces, quantum electrodynamics, and computational electromagnetics.